Chemical Science

ROYAL SOCIETY OF CHEMISTRY

EDGE ARTICLE

View Article Online
View Journal | View Issue

Cite this: *Chem. Sci.*, 2021, **12**, 5473

All publication charges for this article have been paid for by the Royal Society of Chemistry

Received 24th February 2021
Accepted 9th March 2021

DOI: 10.1039/d1sc01098k

rsc.li/chemical-science

DNA-based constitutional dynamic networks as functional modules for logic gates and computing circuit operations†

Zhixin Zhou, [a] Jianbang Wang,[a] R. D. Levine,[a] Francoise Remacle[b] and Itamar Willner *[a]

A nucleic acid-based constitutional dynamic network (CDN) is introduced as a single computational module that, in the presence of different sets of inputs, operates a variety of logic gates including a half adder, 2 : 1 multiplexer and 1 : 2 demultiplexer, a ternary multiplication matrix and a cascaded logic circuit. The CDN-based computational module leads to four logically equivalent outputs for each of the logic operations. Beyond the significance of the four logically equivalent outputs in establishing reliable and robust readout signals of the computational module, each of the outputs may be fanned out, in the presence of different inputs, to a set of different logic circuits. In addition, the ability to intercommunicate constitutional dynamic networks (CDNs) and to construct DNA-based CDNs of higher complexity provides versatile means to design computing circuits of enhanced complexity.

Introduction

The use of DNA as a functional material for logic gate operations and computational circuitry has attracted substantial research efforts in the past two decades.[1–4] Data storage, retrieval and random access of information by DNA strands,[5–8] and the use of DNA assemblies as functional *in vivo* operating computing circuitry, were extensively discussed.[9–11] The structural and functional information encoded in the base sequences of nucleic acids, and the possibility to reconfigure nucleic acid structures by auxiliary input triggers such as pH,[12–14] metal ions,[15–17] fuel strands,[18,19] molecular or macromolecular ligands[20,21] and DNA machines[22,23] enabled the design of logic gates of variable complexities. In addition, by applying the strand displacement mechanism,[24–26] the programmed cleavage of DNA templates by enzymes[27,28] and the catalytic functions of nucleic acids (DNAzymes),[29–32] complex nucleic acid-based computing circuitries and cascaded logic gates were demonstrated. Furthermore, the catalytic properties of nucleic acids provided powerful units as output transduction modules of logic gate cascades and computing circuitry operations.[33–35] However, the processing and scaling of DNA computing systems are still challenging issues. Past efforts addressed these problems by designing reversible logic gates,[36,37] switching circuits,[38] continuous multivalued logic,[39] multiplexer–demultiplexer systems[40,41] and the construction of multilayer input–output logic gates.[42–44] Also, the use of two-dimensional and three-dimensional DNA objects revealing shape complementarity or localized signal propagation could provide means to enhance computational efficacy.[45–47]

Nucleic acid-based constitutional dynamic networks, CDNs, attract substantial research efforts as a means to mimic biological networks.[48] The simplest [2 × 2] CDN consists of four two-component equilibrated constituents *AA′*, *AB′*, *BA′* and *BB′*.[49,50] The stabilization of one of the constituents, *e.g.*, *AA′*, results in the adaptive reconfiguration of the CDN into a new equilibrated network where the constituent *AA′* is upregulated (enriched in its content) at the expense of the constituents that share components with *AA′*, *e.g.*, *AB′* and *BA′*, that are separated to enrich *AA′*. The separated constituents lead to the formation of *B* and *B′* that recombine. Thus, the upregulation of *AA′* is accompanied by the downregulation of *AB′* and *BA′*, and the concomitant upregulation of the constituent that does not share components with *AA′*, *e.g.*, *BB′*. The base sequence comprising nucleic acid offers substantial structural and functional information that provides means to construct and operate the dynamic functions of CDNs. The stability of duplex nucleic acids is dictated by the number and nature of base pairs comprising the duplexes.[51–53] In addition, the formation of DNA triplexes[54] or G-quadruplexes[55,56] and the intercalation of photoisomerizable intercalators into double stranded nucleic acids,[57–59] provide versatile means to control the stability of DNA structures. Furthermore, functional information encoded in nucleic acid structures include catalytic properties (DNAzymes).[60–62] By the conjugation of catalytic nucleic acids to the

[a]*The Institute of Chemistry, The Hebrew University of Jerusalem, Jerusalem 91904, Israel. E-mail: Itamar.willner@mail.huji.ac.il*

[b]*Theoretical Physical Chemistry, UR MolSys B6c, University of Liège, B4000 Liège, Belgium*

† Electronic supplementary information (ESI) available. See DOI: 10.1039/d1sc01098k

CDN constituents, catalytic readout units can be integrated into the constituent structures, and these act as transducing outputs that follow the input-driven dynamic reconfiguration transition of the CDNs. Indeed, in a series of recent reports the input-driven dynamic reconfiguration of nucleic acid-based CDNs were introduced. The adaptive reconfiguration of CDNs using fuel strands,[63] guided formation of K^+-ion-stabilized G-quadruplexes,[64] formation of triplex structures[65] and the application of photoisomerizable azobenzene modules and light[66] was demonstrated. By coupling Mg^{2+}-ion-dependent DNAzyme units, optical (fluorescence) transducing reporter outputs that follow the dynamic transitions of the CDNs were established. The nucleic acid-based CDNs were used to mimic native dynamic networks by providing the intercommunication of CDNs,[65] feedback-driven CDNs,[64] the assembly of networks of enhanced complexities, *e.g.*, [3 × 3] CDNs[67] and three-dimensional CDNs.[68] The application of CDNs is, however, a challenging topic. CDNs were applied as functional modules to design hydrogel materials of switchable stiffness properties,[69] to regulate and switch the aggregation and catalytic properties of nanoparticles,[70] and to control the dimerization of DNA tetrahedra structures as models for protein–protein interactions.[71] The intrinsic features of CDNs to be triggered by auxiliary input triggers and the ability to readout the state (composition) of the CDNs by catalytic DNAzyme output signals suggest the CDNs could provide a module for logic operation and the design of computing circuits.

Here we wish to introduce a single CDN module that, in the presence of appropriate auxiliary inputs, behaves like a reprogrammable logic unit that can be reconfigured to operate as a half-adder, a 2 : 1 multiplexer and 1 : 2 demultiplexer, a ternary multiplication matrix and a cascaded logic circuit. The fact that the AND and XOR gates operate, in parallel, in the single CDN module of the half adder (or in the general map of CDN responses on switches acting in series or in parallel) implies that the CDNs modules provide a universal set of gates. Namely, any Boolean function (of two variables) can be computed with the same CDN module using different triggers as inputs. Besides demonstrating the versatility of logic gates and computing circuits, the use of CDNs as computing module introduces a unique feature reflected by the transduction of each of the operating gates by four parallel output signals provided by the four constituents. This redundant output represents a significant robustness, reliability and accuracy of the readout outputs. Furthermore, the four parallel outputs may be utilized to fan-out the information generated by the computation module to form diverse computing circuits outlined in Scheme 1.

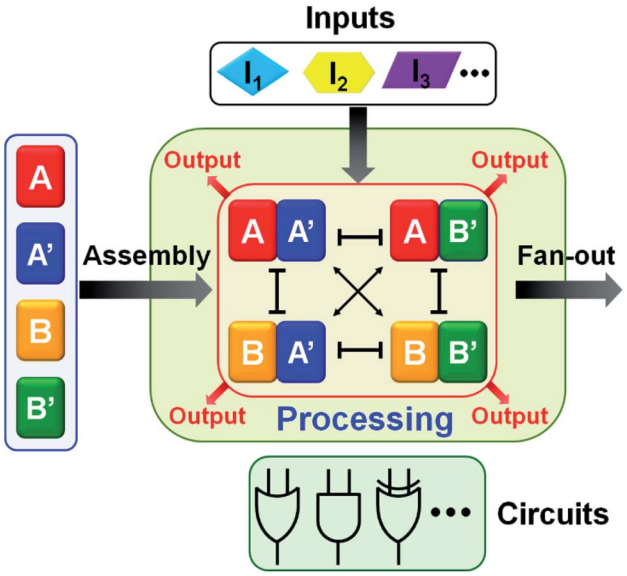

Scheme 1 A constitutional dynamic network, CDN, acting as a functional module for information processing. *A*, *A*′, *B* and *B*′ represent components; *AA*′/*BB*′ and *AB*′/*BA*′ are agonist constituents (do not share components); *AA*′/*AB*′, *AB*′/*BB*′, *BB*′/*BA*′ and *BA*′/*AA*′ are antagonist constituents (share components).

Results and discussion

One CDN-based logic gate system operating as a half-adder is displayed in Fig. 1. It consists of CDN "*X*" that is composed of the four constituents *AA*′, *AB*′, *BA*′ and *BB*′. Each of the constituents includes duplex domains conjugated to single strand loops in each of the components. To the loop strands are associated with single strand tethers, *a*, *a*′, *b*, and *b*′, that yield "arms", *a*/*a*′, *a*/*b*′, *b*/*a*′ and *b*/*b*′ conjugated to the constituents *AA*′, *AB*′, *BA*′ and *BB*′, respectively. In addition, the components of the duplex domains associated with the four constituents are further conjugated to single strand tethers that allow further dictated hybridization with auxiliary strands. The double-loop domains extended by the respective arms *a*/*a*′, *a*/*b*′, *b*/*a*′ and *b*/*b*′ form the Mg^{2+}-ion-dependent DNAzyme assemblies that can recognize four different fluorophore (F_i)-/quencher (Q_i)-functionalized substrates (S_i). The cleavage of these substrates leads

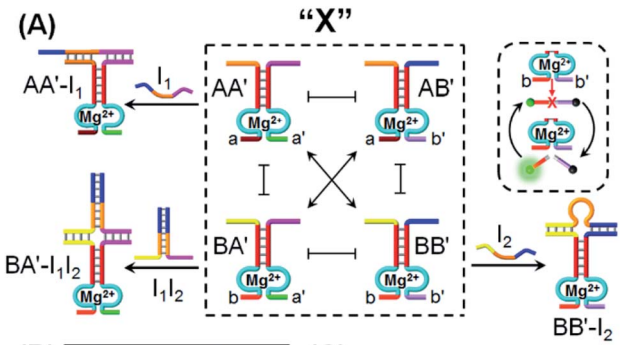

(B)

Inputs		Outputs	
I_1	I_2	AA'	AB'
0	0	0	0
1	0	1	0
0	1	1	0
1	1	0	1

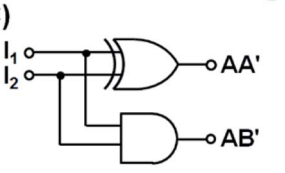

Fig. 1 (A) Schematic CDN-guided operation as a half-adder. (B) Truth-table of the CDN half-adder driven by I_1 and I_2 as inputs and the reporter units associated with constituents *AA*′ and *AB*′ as outputs. (C) Scheme of the half-adder logic gate driven by the CDN.

to the triggered formation of the respective fluorescence, F_i. By following the time-dependent fluorescence changes of each of the fluorophores, and using appropriate calibration curves generated by different concentrations of the intact, separate constituents, the contents of the each of constituents in CDN "*X*" could be quantitatively evaluated. The contents of the constituents in the equilibrated CDN "*X*" are controlled by the relative stabilities of the constituents. The operation of the CDN "*X*" as a logic gate module is displayed in Fig. 1A by subjecting the CDN to the strands I_1 or/and I_2 as inputs. Treatment of the CDN "*X*" with input I_1 results in its hybridization to the arms of *AA*′. The stabilization of the constituents (*AA*′–I_1) reconfigures the CDN by the upregulation of *AA*′, the concomitant upregulation of *BB*′ and the downregulation of *AB*′ and *BA*′. Subjecting the CDN "*X*" to the input I_2 leads to the stabilization of the constituent *BB*′ in the form of *BB*′–I_2, and thus reconfigures the CDN into a new equilibrated configuration where *BB*′ is upregulated with the concomitant upregulation of *AA*′, and the downregulation of the constituents *AB*′ and *BA*′. The two triggered inputs I_1 and I_2 are, however, pre-engineered to interhybridize into a duplex structure that includes two single-stranded arms capable of hybridizing with the free arms associated with the constituent *BA*′. Thus, subjecting the CDN "*X*" to the two inputs I_1 and I_2 results in the hybridization of duplex I_1I_2 to the constituent *BA*′. The association and stabilization of constituent *BA*′ in the form of *BA*′–I_1I_2 reconfigures the CDN into a newly equilibrated configuration where *BA*′–I_1I_2 is upregulated with the concomitant upregulation of *AB*′ and the downregulation of *AA*′ and *BB*′. The contents of the constituents in the input-triggered reconfigured CDNs provide, then, the output readout signals of the systems. For example, Fig. 1B exemplifies the expected truth table upon the inputs I_1/I_2-driven reconfiguration of the CDN and using the contents of *AA*′ and *AB*′ as output signals for the system (as compared to the original contents of the constituents). Considering the initial contents of *AA*′ and *AB*′ in CDN "*X*" as zero base labels of the outputs and any increased value of these outputs as a true output "1", the truth table demonstrates that in the presence of the input I_1 or I_2, the output *AB*′ corresponds to an "AND" gate whereas the output of *AA*′ corresponds to a "XOR" gate. Thus, the inputs I_1/I_2-driven reconfiguration of the CDN "*X*" module yields a half-adder operation, as schematically presented in Fig. 1C.

In fact, the I_1/I_2-driven reconfiguration of CDN "*X*" yields four logically equivalent pairs of output signals (*vide infra*). Nonetheless, as will be point out, the redundancy of the logically equivalent pairs of outputs introduced reliable readout of the computing module, and each of the equivalent outputs may be fanned out to a different logic circuit by coupling to different inputs. The experimental results demonstrating the parallel operation of the CDN as a functional half-adder system are presented in Fig. 2. Fig. 2A shows the time-dependent fluorescence changes generated by the Mg^{2+}-ion-DNAzyme reporter units associated with the constituents of CDN "*X*" before subjecting the system to input I_1, curves (i), and after the equilibration of the CDN in the presence of input I_1, curves (ii). As expected, the fluorescence changes generated by the reporter units linked to *AA*′ and *BB*′ are upregulated by (49% and 30%,

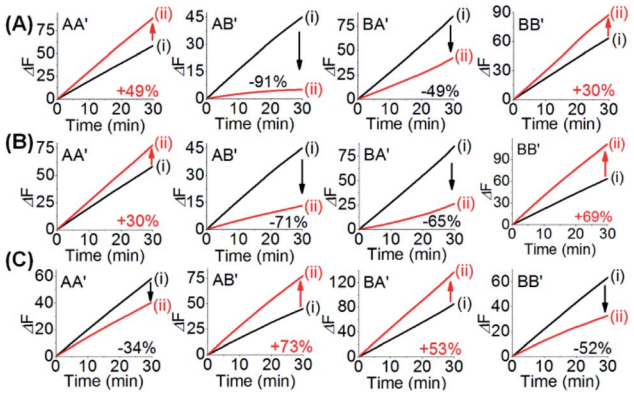

Fig. 2 Time-dependent fluorescence changes generated by the reporter units associated with the constituents of CDN "*X*": (A) Before subjecting to input I_1 (i) and after treatment with input I_1 (ii); (B) before subjecting to input I_2 (i) and after treatment with input I_2 (ii); (C) before subjecting to inputs I_1I_2 (i) and after treatment with inputs I_1I_2 (ii).

respectively) whereas the fluorescence changes of the reporter units conjugated to *AB*′ and *BA*′ are downregulated (by 91% and 49%). Similarly, Fig. 2B depicts the time-dependent fluorescence changes generated by the reporter units associated with CDN "*X*" before (curves (i)) and after (curves (ii)) the treatment of the CDN "*X*" with input I_2. As explained, the fluorescence changes generated by the reporter units linked to *AA*′ and *BB*′ are enhanced by 30% and 69%, while the fluorescence outputs of *AB*′ and *BA*′ are downregulated by 71% and 65%, respectively. Fig. 2C shows the fluorescence changes transduced by the reporter units linked to the constituents upon reequilibration of the CDN, in the presence of the two inputs I_1 and I_2. Under these conditions, the time-dependent fluorescence changes generated by the reporter units associated with the constituents reveal the downregulation of *AA*′ (34%) and *BB*′ (52%), as compared to the fluorescence intensities of these reporter units prior to the intervention with the inputs. In turn, the I_1I_2-driven downregulation of the fluorescence intensities of *AA*′ and *BB*′, is accompanied, as expected, by the concomitant upregulation of the fluorescence intensities of *AB*′ and *BA*′ by 73% and 53%, respectively. The time-dependent fluorescence changes generated by the Mg^{2+}-ion-dependent DNAzyme reporter units before treatment of CDN "*X*" with the inputs, and after subjecting of the CDN to the respective inputs were translated into the quantitative contents of the constituents. For this purpose, appropriate calibration curves relating to the fluorescence changes generated by variable concentrations of intact, separated, constituents were derived, Fig. S1 and S2.† The contents of the constituents in the different states of the CDN are summarized in Fig. S3.† (For the sensitivity of the reporter units to concentration changes of the input, and thus to possible errors of the computational module see Fig. S4† and accompanying discussion). Furthermore, it should be noted that the degrees of upregulation and downregulation of the four constituents differ in their magnitudes. This is consistent with the fact that the constituents in their initial states differ in their equilibrated concentrations and these values are dictated by the

relative stabilities of the constituents. The degrees of upregulation/downregulation are, also, determined by the relative stabilities of the constituents.

Fig. 3A depicts the concentrations of the *AA′* and *AB′* in the presence of a "bar" presentation. Using the contents of the constituents in CDN "*X*" as a threshold value to evaluate the output signals, one may realize that the output of *AA′* corresponds to a XOR gate, while the output of *AB′* corresponds to an "AND" gate, and the two outputs of the CDN yield the parallel half-adder operation. (For further support on the parallel readout of the half-adder operation by electrophoretic measurements, see Fig. S5† and accompanying discussion). The discussion has exemplified the parallel half-adder operation of the CDN by applying the responses of *AA′* and *AB′* as outputs of the half-adder. Nonetheless, by using the readout signals of the other constituents of the CDN as outputs, one may formulate the truth table shown in Fig. S3A,† demonstrating that the I_1/I_2-driven operation of the CDN yields the parallel generation of four pairs of logically equivalent output signals for the same half-adder Fig. 3B. These results demonstrate the unique and important features of CDNs for operating logic gate circuitry. The CDN "*X*" does not only provide an integrated module for the operation of a half-adder, but introduces a functional unit that yields four logically equivalent pairs of output signals for a single half-adder. In addition, this result is not only important as a path to reduce the error of the circuit output, but it introduces a means to fan out the CDN to four subsequent cascaded CDNs, Fig. S3B.†

In the next step, we applied CDN "*X*" that previously used as the functional module to drive, in the presence of appropriate inputs, a set of half-adders, to operate, in the presence of other tailored inputs, the 1 : 2 multiplexer and the 2 : 1 demultiplexer logic systems. Multiplexer/demultiplexer logic operations represent routes for data compression/decompression.[40] The 2 : 1 multiplexer selects and directs, in the presence/absence of a selector, two inputs into one output. On the other hand, the 1 : 2 demultiplexer transforms, in the presence/absence of the selector, one input into two dictated outputs. Fig. 4A introduces the use of CDN "*X*" as a 2 : 1 multiplexer system. In the presence of the input I_3 that stabilizes the constituent *BA′*, the constituent *BA′* is upregulated, the constituents *AA′* and *BB′* are downregulated and the constituent *AB′* is concomitantly upregulated. Subjecting the CDN "*X*" to input I_4 leads to the stabilization and upregulation of *BB′*, the concomitant upregulation of *AA′* and the downregulation of *AB′* and *BA′*. The input I_4 is, however, engineered to hybridize with I_3 and the hybrid I_3I_4 stabilizes constituent *BA′*. As a result, in the presence of the two inputs I_3I_4, *AB′* and *BA′* are upregulated whereas *AA′* and *BB′* are downregulated. These reconfigurations proceed, however, in

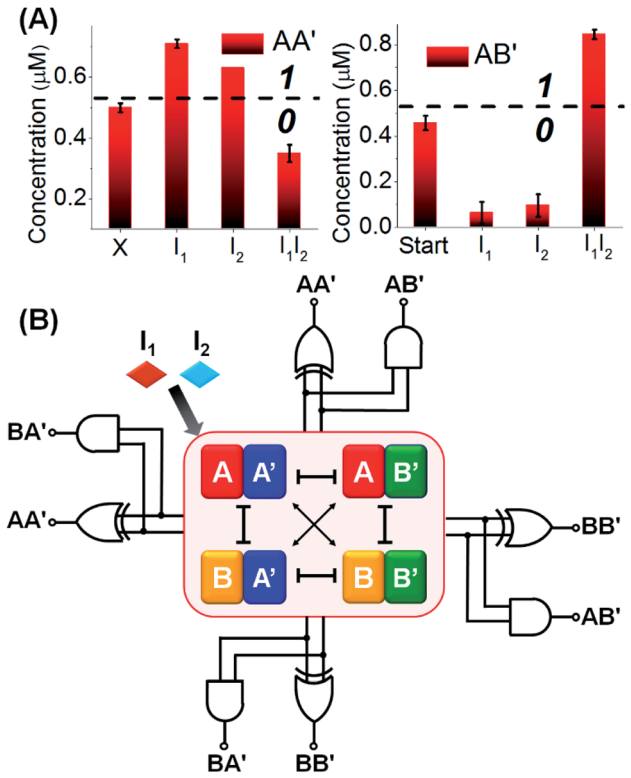

Fig. 3 (A) Content changes generated by the reporter units associated with constituents *AA′* and *AB′* acting as outputs in the form of a bar presentation. Error bars derived from $N = 3$ experiments. (B) Schematic operation of the CDN "*X*" as functional unit leading to four logically equivalent pairs of output signal of a single half adder using I_1 and I_2 as inputs: (*AA′*, *AB′*), (*AA′*, *BA′*), (*BB′*, *AB′*) and (*BB′*, *BA′*).

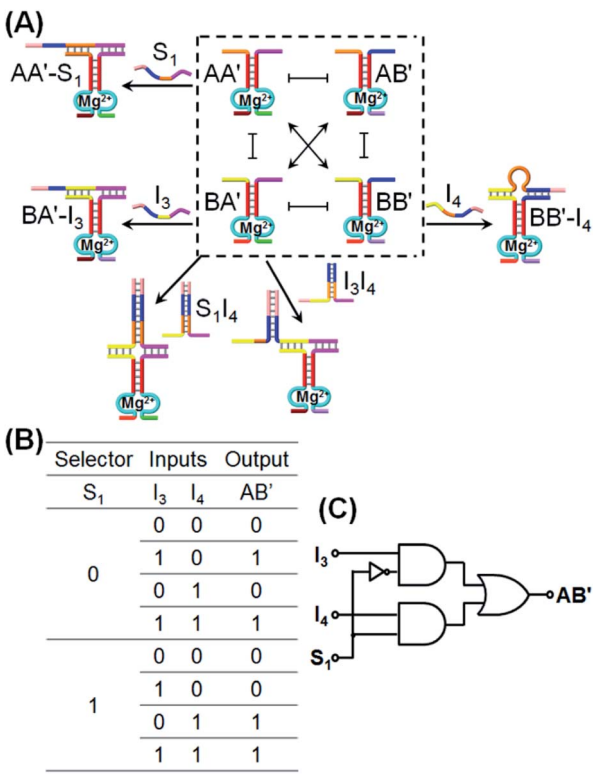

Fig. 4 Schematic CDN-guided operation of a 2 : 1 multiplexer logic gate. (B) Truth-table corresponding to the CDN 2 : 1 multiplexer driven by the inputs I_3 and I_4 and the selector S_1 using the content changes generated by the DNAzyme reporter units associated with *AB′* as output. (C) Scheme of the 2 : 1 multiplexer logic operation driven by the inputs/selector and transduced by the constituent *AB′* as output.

the absence of the selector S_1. Treatment of the CDN "*X*" with the selector S_1 results in the stabilization and upregulation of *AA*′ and *BB*′ and the downregulation of *AB*′ and *BA*′. In the presence of S_1 and I_3, two counter-acting processes take place in the CDN "*X*", where S_1 binds to *AA*′ and I_3 stabilizes the orthogonal constituent *BA*′! As a result, the S_1 and I_3 have counter effects on the reconfiguration of the CDN, and in the presence of S_1 and I_3, no significant changes in the contents of the constituents occurs. In turn, S_1 is pre-engineered to hybridize with I_4, and thus subjecting the CDN to S_1 and I_4 results in the hybridization of the hybrid S_1I_4 with constituent *BA*′, leading to the stabilization and upregulation of *BA*′, the concomitant up-regulation of *AB*′, and the downregulation of *AA*′ and *BB*′. In addition, in the presence of S_1, I_3 and I_4, the hybrid S_1I_4 will stabilize constituent *BA*′, and I_3 will also stabilize *BA*′. Thus, *BA*′ and *AB*′ will be upregulated, and *AA*′ and *BB*′ will be downregulated. According to these details, subjecting CDN "*X*" to the inputs I_3 and/or I_4 and selector S_1, and using the responses of the DNAzyme reporter unit associated with *AB*′ as output, the CDN logic module will perform a 2 : 1 multiplexed operation as summarized in the truth table, Fig. 4B, and schematically presented in Fig. 4C. The experimental results validating the 2 : 1 logic operation using *AB*′ as output, are summarized in Fig. S6–S12, ESI.† The time-dependent fluorescence changes generated by the reporter associated with *AB*′, upon subjecting the CDN "*X*" to the different selector/inputs, and using the appropriate calibration curves, are translated to the contents of the output, and tabulated in the form of a bar presentation, Fig. S13,† confirming that the CDN module operates, indeed, as a 2 : 1 multiplexer. Note, however, that the CDN module includes four constituents, where each constituent could act as the output, and thus, the 2 : 1 multiplexer is read out, in parallel, by four logically redundant outputs. These results are displayed in Fig. S6–S12,† in the form of the different time-dependent fluorescence changes of the reporter units associated with the different output constituents, and in the form of a bar presentation corresponding to the contents of the output constituents. The functions of the CDN "*X*" as a 2 : 1 multiplexer was further supported by electrophoretic imaging, see Fig. S14† and accompanying discussion.

Similarly, the CDN "*X*" was applied as a module that triggers the 1 : 2 demultiplexer logic operation, Fig. 5. This logic system transforms one input into two outputs and is exemplified with the treatment of CDN "*X*", in the presence or absence of a selector S_2, with input I_5. The input I_5 stabilizes the constituent *BB*′ and leads to the reconfiguration of CDN "*X*" into an equilibrated system where *BB*′ is upregulated and concomitantly *AA*′ is upregulated and the constituents *AB*′ and *BA*′ are downregulated. Subjecting CDN "*X*" to the selector S_2 results in the hybridization with component *A*′ in constituent *AA*′ or *BA*′, but this hybridization process has no effect on the stability of *AA*′ and *BA*′, and thus, CDN "*X*" is not affected and none of the constituents is upregulated or downregulated. The selector S_2 and input I_5 are, however, pre-engineered to interhybridize to a hybrid, S_2I_5 that binds to the constituent *BA*′. Thus, subjecting CDN "*X*" to the selector S_2 and input I_5 results in the stabilization of *BA*′, the concomitant upregulation of *AB*′ and the

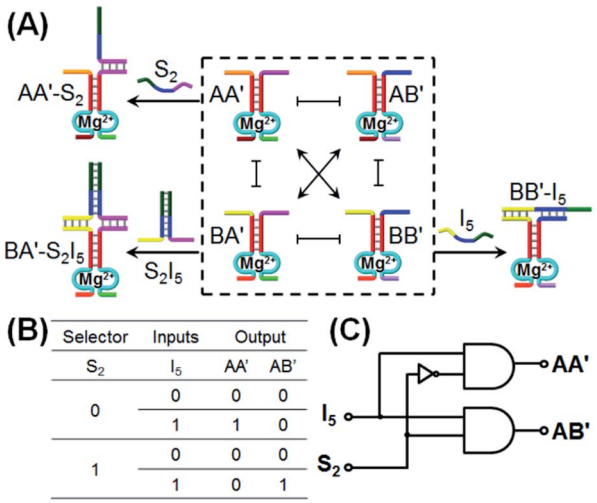

Selector	Inputs	Output	
S_2	I_5	AA'	AB'
0	0	0	0
	1	1	0
1	0	0	0
	1	0	1

Fig. 5 Schematic CDN-guided operation of a 1 : 2 demultiplexer logic gate. (B) Truth-table corresponding to the CDN 1 : 2 demultiplexer driven by the input I_5 and the selector S_2 using the content changes generated by the DNAzyme reporter units associated with *AA*′ and *AB*′ as outputs. (C) Scheme of the 1 : 2 demultiplexer logic operation driven by the input/selector and transduced by the constituent *AA*′ and *AB*′ as outputs.

downregulation of *AA*′ and *BB*′. Using the constituents *AA*′ and *AB*′ as outputs, the formulated truth-table in Fig. 5B follows a 1 : 2 demultiplexer logic operation where one input I_5 generated two outputs, *e.g.*, one output of *AA*′ increases, in the presence of I_5, while a second output of *AB*′ proceeds, in the presence of S_2 and I_5. The schematic 1 : 2 demultiplexer logic is presented in Fig. 5C.

The experimental results demonstrate the CDN-stimulated performance of the 1 : 2 demultiplexer are presented in Fig. 6, where the time-dependent fluorescence changes of DNAzyme reporter units associated with the four constituents upon

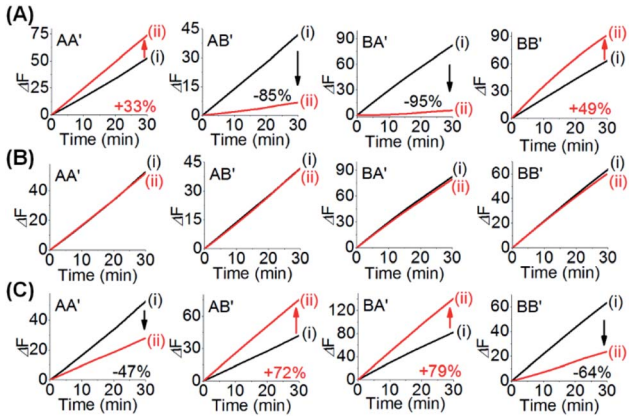

Fig. 6 Time-dependent fluorescence changes generated by the reporter units associated with the constituents of CDN "*X*": (A) before subjecting to input I_5 (i) and after treatment with input I_5 (ii); (B) before subjecting to selector S_2 (i) and after treatment with selector S_2 (ii); (C) before subjecting to input/selector S_2I_5 (i) and after treatment with input/selector S_2I_5 (ii).

subjecting the CDN "*X*" to the different inputs, are displayed. Subjecting the CDN to input I_5, Fig. 6A, results in the upregulation of the reporter units associated with *AA*′ (by 33%), the downregulation of *AB*′ and *BA*′ by 85% and 95% and the concomitant upregulation of *BB*′ (by 49%). Thus, the output of *AA*′, is, "1", whereas the output of *AB*′ is "0". Fig. 6B depicts the time-dependent fluorescence changes of the reporter units associated with the constituents upon subjecting the CDN to the selector S_1. No significant fluorescence changes after applying the selector on the CDN is observed, implying that the outputs of *AA*′ and of *AB*′ are "0" (as well as for all other constituents), consistent with the 1 : 2 demultiplexer operation. Fig. 6C shows the time-dependent fluorescence changes of all four reporter units associated with the CDN upon subjecting the CDN to the selector S_2 and input I_5 (the output *AA*′ is downregulated by 47%, output "0" whereas output *AB*′ is upregulated by 72%, output "1"). These outputs are consistent with the performance of CDN "*X*", and *AA*′ and *AB*′ as outputs, as a logic 1 : 2 demultiplexer. In addition, the constituent *BB*′ is downregulated by 64%, while the constituent *BA*′ is upregulated by 79%. Using the appropriate calibration curves relating the time-dependent fluorescence changes of the reporter units to different concentrations of the intact constituents, the quantitative contents of the constituents were evaluated, Fig. S15.† The contents of the constituents in the CDN "*X*", in the presence of the respective input/selector, can be used for the quantitative evaluation of the output values. For example, Fig. 7A depicts in the form of a bar presentation, the use of the contents of *AA*′ and *AB*′ as constitutive outputs that follow the 1 : 2 demultiplexer operation of the system. It should be noted that the functions of the CDN "*X*" as a 1 : 2 demultiplexer can be followed by electrophoretic imaging of the constituents of the CDN before and after treatment with I_5, S_2 and S_2I_5 (for a detailed description of these results see Fig. S16† and accompanying discussion). In addition, we note that the operation of CDN "*X*" as a 1 : 2 demultiplexer has applied the responses of the reporter units associated with the constituents *AA*′ and *AB*′ as outputs. The results shown in Fig. 6 indicate, however, that one can read in parallel the redundant outputs *AA*′/*BA*′, *BB*′/*AB*′ and *BB*′/*BA*′ for the 1 : 2 demultiplexer system, Fig. 7B and S15.† Thus, the redundancy of the output signals of the CDN "*X*"-based demultiplexer system reemphasizes the possibility to fan out the demultiplexer circuit to other CDNs and thereby demonstrates the minimization of the readout error of the demultiplexer system.

Beyond the ability to use the CDN "*X*" as a functional module that operates half-adder, 2 : 1 multiplexer and 1 : 2 demultiplexer, we demonstrate that, in the presence of appropriate input triggers, the same CDN "*X*" activates a 3 × 3 ternary multiplication matrix.[72] Fig. 8A introduces the CDN "*X*" and the respective inputs that interact with CDN "*X*" to operate the 3 × 3 multiplication matrix. Four inputs $I_{A[+1]}$, $I_{B[+1]}$, $I_{A[-1]}$ and $I_{B[-1]}$ are used to interact with the CDN "*X*" system. Each of these inputs includes an "arch-like" strand configuration that hybridizes with the respective constituents. Nonetheless, the hybridization processes do not affect the stabilities of the constituents of the CDN "*X*", since they hybridize with only one

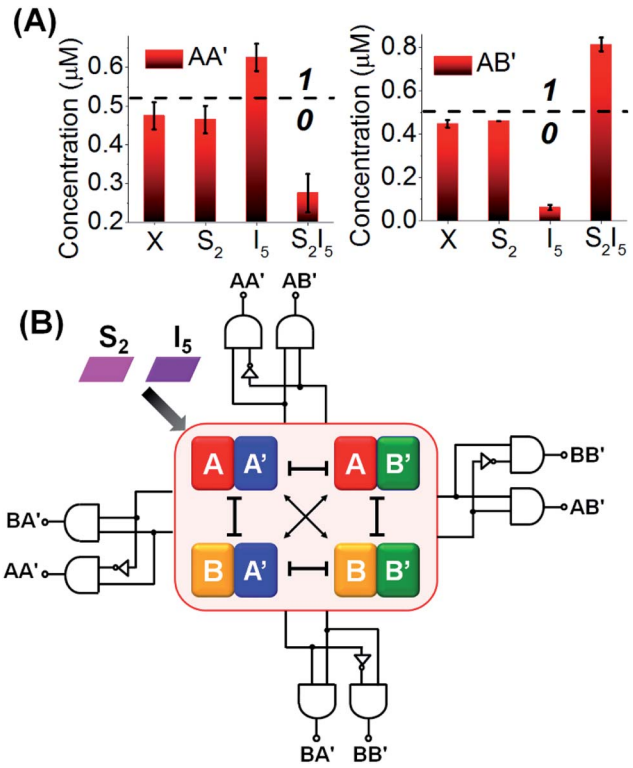

Fig. 7 (A) Bar operation of the content outputs of the 1 : 2 demultiplexer logic gates using the corresponding input and selector. "*X*" stand for the initial contents of the outputs in CDN "*X*" in the absence of any input/selector. Dashed line corresponds to the threshold contents for evaluating the output values. Error bars derived from $N = 3$ experiments. (B) Schematic operation of CDN "*X*" as a functional unit to form four different logically redundant pairs of output signal of a single 1 : 2 demultiplexer in the presence of input I_5 and selector S_2.

"arm" of the constituents and, thus, do not reconfigure the CDN. Hence, the DNAzyme reporter units associated with the constituents are not affected by the inputs, $[-1] \times [0] = 0$ and $[+1] \times [0] = 0$. The inputs are, pre-engineered to yield interhybridized pairs that stabilize the four constituents of CDN "*X*", and can be considered as products of the multiplication matrix, *e.g.*, $I_{A[+1]}I_{B[+1]}$ stabilizes *AA*′; $I_{A[-1]}I_{B[+1]}$ stabilizes *BA*′; $I_{A[+1]}I_{B[-1]}$ stabilizes *AB*′ and $I_{A[-1]}$ $I_{B[-1]}$ stabilizes *BB*′, Fig. 8B. Assuming that the output of the 3 × 3 multiplication matrix is the readout signal of the reporter unit associated with the constituent *AA*′, the treatment of the CDN "*X*" with $I_{A[+1]}I_{B[+1]}$ will upregulate *AA*′, output "1"; treatment of the CDN "*X*" with $I_{A[-1]}I_{B[-1]}$ stabilizes *BB*′ and, concomitantly, *AA*′, thus, leading to the output "1", $[-1] \times [-1] = 1$ and $[+1] \times [+1] = 1$. Subjecting the CDN to the inputs $I_{B[-1]}I_{A[+1]}$ or $I_{B[+1]}I_{A[-1]}$ stabilizes the constituents *AB*′ and *BA*′, respectively, resulting in their upregulation and the concomitant downregulation of *AA*′ and *BB*′. As a result, the output signal of *AA*′ in the presence of these two products will be downregulated, as compared to the original output value of *AA*′, prior to the interaction with these input products, output "−1" and "−1", respectively, $[-1] \times [+1] = -1$ and $[+1] \times [-1] = -1$.

Fig. 9 depicts the experimental time-dependent fluorescence changes of the output *AA*′ reporter unit, upon subjecting the

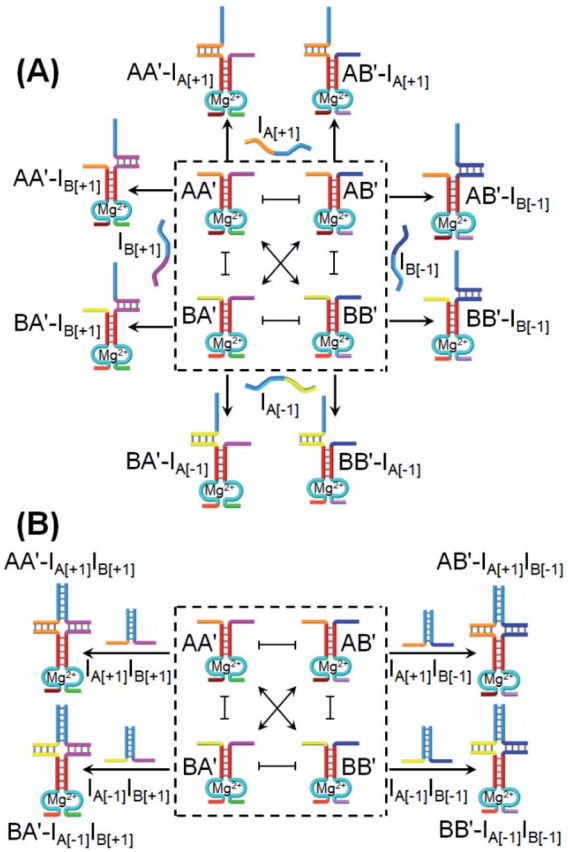

Fig. 8 Application of CDN "*X*" as a computational module operating as a ternary 3 × 3 multiplication matrix. (A) Modes of interaction of the four individual inputs $I_{A[+1]}$, $I_{B[+1]}$, $I_{A[-1]}$, and $I_{B[-1]}$ with the constituents comprising CDN "*X*". (B) Models of interaction of combination of two inputs, $I_{A[+1]}I_{B[+1]}$, $I_{A[-1]}I_{B[-1]}$, $I_{A[+1]}I_{B[-1]}$, and $I_{A[-1]}I_{B[+1]}$ with the constituents of CDN "*X*".

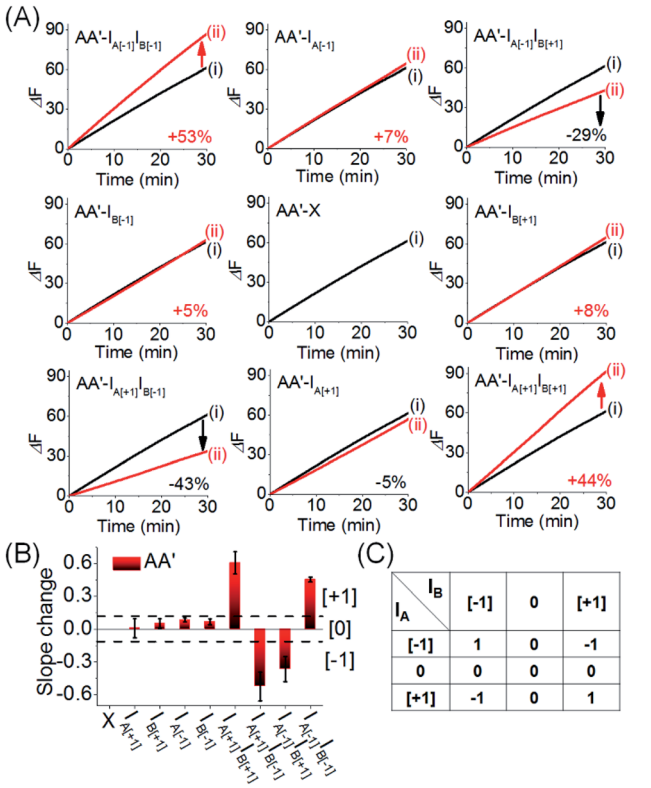

Fig. 9 (A) Time-dependent fluorescence changes generated by the reporter unit associated with *AA*′ upon subjecting CDN "*X*" to the different inputs outlined in Fig. 8. Curves (i) correspond to the response of the *AA*′ reporter unit before the application of any inputs, curves (ii) correspond to the results of applying different inputs. For the time-dependent fluorescence changes of the reporter units associated with the other three constituents see ESI Fig. S17A–S19A.† (B) Bar presentation of the fluorescence changes associated with the constituent *AA*′ in the presence of the different inputs. Error bars derived from $N = 3$ experiments. (C) Truth-table corresponding to the ternary 3 × 3 multiplication matrix generated by *AA*′ (for the bar presentation of the fluorescence changes associated with the other three constituents and the comprehensive 3 × 3 multiplication matrix generated by all of the constituents of the CDN "*X*", see Fig. S17B–S19B†).

CDN "*X*" to the respective pairs of input products, in comparison to the time-dependent fluorescence changes generated by the reporter unit associated with *AA*′ prior to interaction to the products inputs. As expected, subjecting the CDN "*X*" to the products $I_{A[-1]}I_{B[-1]}$ and $I_{A[+1]}I_{B[+1]}$ leads to the upregulation of the output signal of *AA*′ by 53% and 44%, respectively, output "+1", whereas the interaction of $I_{A[-1]}$ $I_{B[+1]}$ and $I_{B[-1]}$ $I_{A[+1]}$ leads to the downregulation of the *AA*′ output by −29% and −43%, respectively, resulting in of "−1" output. The 3 × 3 multiplication matrix generated upon subjecting CDN "*X*" to the set of inputs summarized in a form of a "bar" presentation in Fig. 9B. Using the domain of percentage changes in the region of +0.12 to −0.12 as threshold of "0" output of the reporter unit, the percentage changes above or below the threshold values are defined as "+1" or "−1", respectively, Fig. 9B, and the respective truth table, Fig. 9C. Note, however, that the 3 × 3 ternary multiplication matrix used the reporter associated with *AA*′ as output. In principle, the responses of the three reporters associated with the other three constituents could also be "outputs" for the same multiplication matrix, thus enhancing the reliability of the computation circuit (time-dependent fluorescence changes of the reporter units associated with the different output constituents, bar presentation corresponding to the contents of the output constituents, and electrophoretic image, see Fig. S17–S20†).

Finally, we applied CDN "*X*" to operate a logic circuitry consisting of an AND–InhibitAND cascade, Fig. 10. The first layer of the cascade includes the AND gate, where the activity of the DNAzyme reporter unit associated with *AB*′ provides the output signal of the entire cascade. Subjecting CDN "*X*" to input I_6 stabilizes constituent *AA*′, leading to the upregulation of *AA*′ and *BB*′, and the downregulation of *AB*′ and *BA*′. Thus, the output signal is lower than the background, threshold, output of the non-treated network, output "0". Similarly, subjecting CDN "*X*" to input I_7, stabilizes constituent *BB*′, leading to its upregulation and to the downregulation of *AB*′, output "0". Treatment of the CDN "*X*" with the two inputs, I_6 and I_7, results in the interbridging of the strands and the resulting duplex I_6I_7 hybridized with *BA*′. The stabilization of *BA*′ is accompanied by

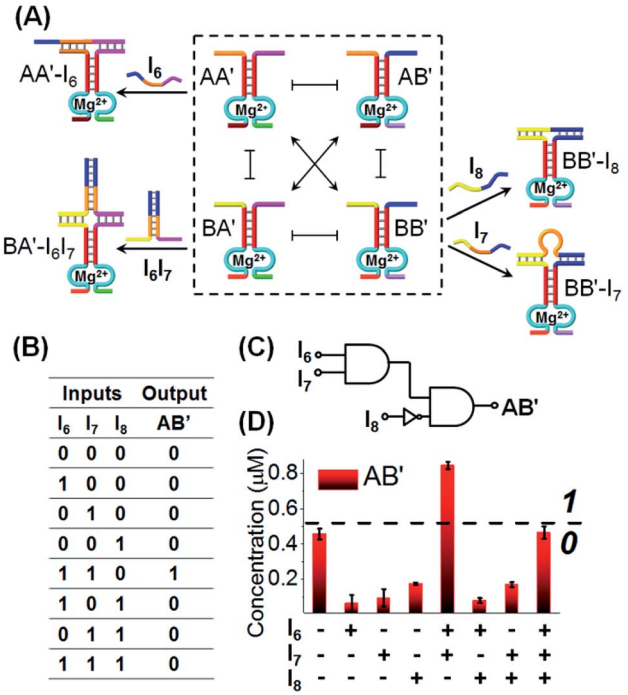

Fig. 10 Schematic CDN-guided operation of AND–InhibitAND cascade circuit. (B) Truth-table corresponding to the CDN AND–InhibitAND cascade driven by the inputs I_6, I_7 and I_8 using the content changes generated by the DNAzyme reporter unit associated with AB' as output. (C) Scheme of the AND–InhibitAND cascade operation driven by the inputs and transduced by the constituent AB' as output. (D) Content changes generated by the reporter units and acting as outputs in the form of a bar presentation. Error bars derived from $N = 3$ experiments.

its upregulation, downregulation of AA' and BB', and the concomitant upregulation of AB'. The upregulation of the output reporter DNAzyme, AB' results in an enhanced output signal, as compared to the original background, threshold signal, output "1". That is, the first layer of the circuitry corresponds to an AND gate using the reporter AB' as output (that is intensified in the presence of I_6I_7). The second layer of the logic cascade includes the coupling of the input I_8 with the CDN "X". The input I_8 hybridizes with the constituent BB' leading to its stabilization and upregulation, and to the concomitant downregulation of the output constituent AB', output "0". The stabilization of the constituent BB' by I_8 and the upregulation of BB' opposes, however, the stabilization of BA' by the inputs I_6I_7. Thus, the stabilization of the constituent BB' is accompanied by the weakening of the output signal of AB', leading to a response of AB' that is below the threshold output of AB' prior to the application of the inputs, output "0". Thus, upon coupling the AB' output of the first layer gate with input I_8 acting as input of the second gate layer leads to a "0" output and the operation of an InhibitAND gate. The expected truth-table of the two layer cascade is displayed in Fig. 10B, and the schematic formation of the AND–InhibitAND cascade is shown in Fig. 10C. The experimental results corresponding to the time-dependent fluorescence changes of all reporter units associated with the constituents of CDN "X", before and after treatment with the inputs I_6, I_7 and I_8 are displayed in Fig. S21–S25, ESI.† Using the appropriate calibration curves, one may evaluate the concentrations of the respective constituents, in the presence of the appropriate combinations of triggers. For example, the content of AB' was used as the output signal to probe the activity of the CDN "X" and the results are presented in the form of a bar presentation in Fig. 10D. The results confirm that the two layer cascade follow an AND–InhibitAND cascade. Note, that our discussion has applied the reporter signal of constituent AB' as output for the AND–InhibitAND cascade. In principle, one may use the reporter units of the other three constituents as outputs for the single AND–InhibitAND cascade circuitry, Fig. S26.† Furthermore, one may realize the versatility and modularity of CDN "X" to operate, in the presence of other inputs, a variety of other cascaded circuitries. For example, we schematically introduce the assembly of AND–OR cascade, Fig. S27.† Furthermore, by applying an additional input I_{12} on the computational module shown in Fig. 10, fan-out capacities of the system were demonstrated, see Fig. S28A–C.† The cascade gates reveal the advantage of using DNA as function material to construct the gates. The possibility to delicately control the inter-nucleic acid hybridization by the number and nature of complementary base-pairs provides a useful means to eliminate "crosstalk" perturbing interactions and yield pure operations of the constituents.

The five examples applying nucleic acid-based CDN for logic operations and computing circuits introduce important features to the area of DNA computing: (i) one CDN system, CDN "X" consisting of only four DNA strands, can be used as a versatile "information processing center", Scheme 2. In the presence of appropriate pre-engineered inputs, a variety of output circuits may be envisaged. (ii) The mapping of the response of the CDN module on AND and XOR gates provides a universal set of gates. (iii) The orthogonal reconfiguration of the four constituents of the CDN enabled the parallel operation of two logic gates in a single CDN module, *e.g.* the AND and XOR gates. (iv) The availability of four constituents in the CDN processing module, where each of the constituents includes a reporter unit, and allows the parallel readout of the processed logic circuit by four pairs of output signals that are logically

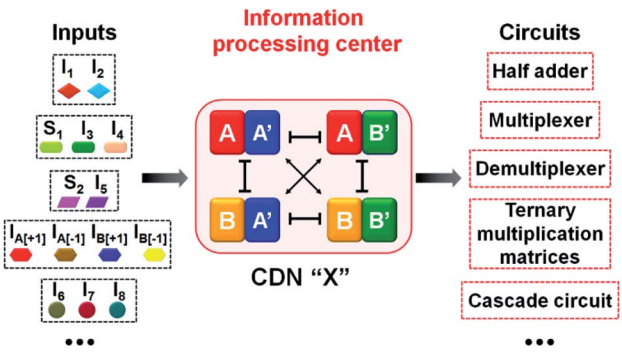

Scheme 2 Summary of an input-triggered CDN that guides the operation of a set of logic gates and computing circuits.

equivalent. This redundancy introduces robustness and a reliable readout of the circuit performance, features that are of particular significance in molecular computing. In addition, the four output signals permit the subsequent fan-out of the information processed CDN module to other CDNs. (v) The demonstrated feasibility to evolve CDNs, to design CDN of increased multiplicity, to tailor CDN revealing feedback-driven reconfiguration, and the design of triggered hierarchically-guided CDNs, provide versatile means to construct logic circuits of enhanced complexities while resolving fundamental computational difficulties, such as signal amplification of weakening cascaded logic pathways.[73,74] (vi) It should be noted that all CDN-guided logic gates and circuits discussed in the paper demonstrated the unidirectional input(s)-guided reconfiguration of the computing module to execute the respective logic operation. Any of the described system can be, however, reset to the original computing module by the addition of the counter input(s), that displace the input(s) associated with the computing modules, without the addition of any other component, except the counter inputs. Considering the fact that the concentrations of the substrates corresponding to the different reporter units exist in excess in the systems, and realizing that the output signals of the reporter units are read-out on a time-scale of 10 to 30 minutes, yet due to the excess of the reporter substrates, the linear fluorescence changes proceed on a time-scale of five hours, the resetting of the computing modules for 5 times should be feasible.

Conclusion

The study introduced the primary application of the CDN concept for DNA logic gate operation. The unique outcome of the study is the demonstration that one common CDN module can be applied as a functional unit, in the presence of different inputs, to activate a set of universal logic gates and logic circuits. The use of the CDN as computational module introduced significant advantages over traditional DNA logic gates and circuits reflected by the generation of four parallel redundant output signals providing computational accuracy and gate stability, and offering fan-out capacity for circuits of enhanced complexities. Realizing the reported complexities of CDNs, *e.g.*, the operation of 3×3 CDNs[67] or three-dimensional CDNs[68] and the control over the hierarchical adaptive reconfiguration of these CDNs, the present study paves means to design future logic gate cascades, fan-in and fan-out gates and more. Furthermore, many natural processes and their outcome are guided by dynamically-driven networks. From a basic scientific view, the present study is inspired by these biological transformations where dynamic changes induced by chemical switching events control the spatiotemporal access to stored information.[75] Thus, beyond the immediate advances introduced by the study to DNA computing systems, it provides, in our opinion, guiding scientific concepts to develop other molecular, macromolecular, or biomolecular computing circuits.

The fact that the CDN is composed of dynamically interchangeable, intercommunicating, constituents that can be triggered by a set of different inputs into a variety of reconfigured compositions provides versatile means to process information. The role of the inputs is to displace the equilibrium between the constituents using Le Chatelier principle,[76] which provides a thermodynamical control for programming the CDNs. In addition, the conjugation of four DNAzyme reporter units acting as outputs for the reconfigured network assembly introduces a general path for the fan-out of the information processed by the CDN module. These unique capabilities of CDNs were successfully applied by introducing a single $[2 \times 2]$ CDN that operated a half-adder, a 2 : 1 multiplexer, a 1 : 2 demultiplexer, a ternary 3×3 multiplication matrix and an AND–InhibitAND cascade. Each of these logic operations and computing circuits was fanned-out into four different outputs, demonstrating the abilities of the CDN to process information. Realizing the fundamental advantages of applying CDNs as functional modules for operating logic gates and computational circuits, one may envisage the further development of the concept: (i) by designing other inputs, other CDN-driven logic gates and logic cascades are feasible. (ii) The input-driven reconfiguration of the CDNs is based on a thermodynamic control. One could now try to manipulate the rate at which the new equilibrium is reached so as to implement time-dependent logic operations. (iii) The ability to evolve and communicate networks[65,73] provides a means to design CDN-guided complex cascaded logic gates and computing circuits. (iv) The present study has applied the simple $[2 \times 2]$ CDN module for logics. Nonetheless, DNA-based CDNs of higher complexity, *e.g.* $[2 \times 3]$ and $[3 \times 3]$ CDNs were designed.[67] This paves principles for indispensable degrees for compression, processing and particularly hierarchically-adaptive computation with CDN modules (for that an discussion on the input-triggered hierarchically adaptive reconfiguration of $[3 \times 3]$ CDNs, see ref. 67)

As for all DNA computing systems, the question of practical applications, and the suggestion of feasible uses of such systems beyond basic science, are still challenges. DNA computing systems are relatively slow and include expensive and sensitive ingredients, and limited recyclability requires the identification of DNA computing assemblies for each target applications. Nonetheless, the interfacing of DNA computing systems with cells for diagnostic and therapeutic application is a natural path to follow. The fact that the computing modules are triggered by nucleic acid inputs, and realizing constituents of the computing modules include catalytic (DNAzyme) counterparts that can be used for the programmed synthesis of sequence-specific output strands suggest various possible theranostic applications of DNA computing devices. For example, triggering of the computing modules by specific miRNA inputs could provide autonomous sensing and detection means of different diseases such as cancer.[77] In addition, the biomarker-input-triggered logic activation of the DNAzyme units could provide versatile means to synthesize programmed sequences such as SiDNA or gene-guided transcription and translation of proteins.[10] Nonetheless, such farseeing vision of DNA coupling will require further advancements and effective means to image the intracellular logic operation.

Conflicts of interest

There are no conflicts to declare.

Acknowledgements

This study is supported by the Israel Science Foundation. FR thanks Fonds National de la Recherche, FRS-FNRS, Belgium, for its support (MONACOMP #T0205.20).

Notes and references

1 I. Willner, B. Shlyahovsky, M. Zayats and B. Willner, *Chem. Soc. Rev.*, 2008, **37**, 1153.
2 T. Fu, Y. Lyu, H. Liu, R. Peng, X. Zhang, M. Ye and W. Tan, *Trends Biochem. Sci.*, 2018, **43**, 547–560.
3 D. Fan, J. Wang, E. Wang and S. Dong, *Adv. Sci.*, 2020, 2001766, DOI: 10.1002/advs.202001766.
4 H. Sun, J. Ren and X. Qu, *Acc. Chem. Res.*, 2016, **49**, 461–470.
5 L. Ceze, J. Nivala and K. Strauss, *Nat. Rev. Genet.*, 2019, **20**, 456–466.
6 G. Gines, A. S. Zadorin, J. C. Galas, T. Fujii, A. Estevez-Torres and Y. Rondelez, *Nat. Nanotechnol.*, 2017, **12**, 351–359.
7 C. Mao, T. H. LaBean, J. H. Reif and N. C. Seeman, *Nature*, 2000, **407**, 493–496.
8 X. Song and J. Reif, *ACS Nano*, 2019, **13**, 6256–6268.
9 J. Li, A. A. Green, H. Yan and C. Fan, *Nat. Chem.*, 2017, **9**, 1056–1067.
10 A. A. Green, J. Kim, D. Ma, P. A. Silver, J. J. Collins and P. Yin, *Nature*, 2017, **548**, 117–121.
11 J. Hemphill and A. Deiters, *J. Am. Chem. Soc.*, 2013, **135**, 10512–10518.
12 T. Li, D. Ackermann, A. M. Hall and M. Famulok, *J. Am. Chem. Soc.*, 2012, **134**, 3508–3516.
13 Y. Hu, A. Cecconello, A. Idili, F. Ricci and I. Willner, *Angew. Chem., Int. Ed.*, 2017, **56**, 15210–15233.
14 H. Pei, L. Liang, G. Yao, J. Li, Q. Huang and C. Fan, *Angew. Chem., Int. Ed.*, 2012, **51**, 9020–9024.
15 T. Li, E. Wang and S. Dong, *J. Am. Chem. Soc.*, 2009, **131**, 15082–15083.
16 K. S. Park, C. Jung and H. G. Park, *Angew. Chem.*, 2010, **122**, 9951–9954.
17 Y. Miyake, H. Togashi, M. Tashiro, H. Yamaguchi, S. Oda, M. Kudo, Y. Tanaka, Y. Kondo, R. Sawa, T. Fujimoto, T. Machinami and A. Ono, *J. Am. Chem. Soc.*, 2006, **128**, 2172–2173.
18 L. Qian, E. Winfree and J. Bruck, *Nature*, 2011, **475**, 368–372.
19 L. Qian and E. Winfree, *Science*, 2011, **332**, 1196–1201.
20 L. Feng, Z. Lyu, A. Offenhäusser and D. Mayer, *Angew. Chem., Int. Ed.*, 2015, **54**, 7693–7697.
21 R. Peng, X. Zheng, Y. Lyu, L. Xu, X. Zhang, G. Ke, Q. Liu, C. You, S. Huan and W. Tan, *J. Am. Chem. Soc.*, 2018, **140**, 9793–9796.
22 J. Bath and A. J. Turberfield, *Nat. Nanotechnol.*, 2007, **2**, 275–284.
23 G. Yao, J. Li, Q. Li, X. Chen, X. Liu, F. Wang, Z. Qu, Z. Ge, R. P. Narayanan, D. Williams, H. Pei, X. Zuo, L. Wang, H. Yan, B. L. Feringa and C. Fan, *Nat. Mater.*, 2019, **19**, 781–788.
24 T. Song, A. Eshra, S. Shah, H. Bui, D. Fu, M. Yang, R. Mokhtar and J. Reif, *Nat. Nanotechnol.*, 2019, **14**, 1075–1081.
25 D. Y. Zhang and E. Winfree, *J. Am. Chem. Soc.*, 2009, **131**, 17303–17314.
26 G. Seelig, D. Soloveichik, D. Y. Zhang and E. Winfree, *Science*, 2006, **314**, 1585–1588.
27 Y. Benenson, B. Gil, U. Ben-Dor, R. Adar and E. Shapiro, *Nature*, 2004, **429**, 423–429.
28 Y. Zhang, Z. Shuai, H. Zhou, Z. Luo, B. Liu, Y. Zhang, L. Zhang, S. Chen, J. Chao, L. Weng, Q. Fan, C. Fan, W. Huang and L. Wang, *J. Am. Chem. Soc.*, 2018, **140**, 3988–3993.
29 J. Elbaz, O. Lioubashevski, F. Wang, F. Remacle, R. D. Levine and I. Willner, *Nat. Nanotechnol.*, 2010, **5**, 417–422.
30 R. Orbach, B. Willner and I. Willner, *Chem. Commun.*, 2015, **51**, 4144–4160.
31 J. Zhang and Y. Lu, *Angew. Chem., Int. Ed.*, 2018, **57**, 9702–9706.
32 S. Bi, Y. Yan, S. Hao and S. Zhang, *Angew. Chem., Int. Ed.*, 2010, **49**, 4438–4442.
33 J. Zhu, L. Zhang, T. Li, S. Dong and E. Wang, *Adv. Mater.*, 2013, **25**, 2440–2444.
34 H. Lederman, J. Macdonald, D. Stefanovic and M. N. Stojanovic, *Biochemistry*, 2006, **45**, 1194–1199.
35 J. Elbaz, F. Wang, F. Remacle and I. Willner, *Nano Lett.*, 2012, **12**, 6049–6054.
36 A. J. Genot, J. Bath and A. J. Turberfield, *J. Am. Chem. Soc.*, 2011, **133**, 20080–20083.
37 R. Orbach, F. Remacle, R. D. Levine and I. Willner, *Proc. Natl. Acad. Sci. U. S. A.*, 2012, **109**, 21228–21233.
38 F. Wang, H. Lv, Q. Li, J. Li, X. Zhang, J. Shi, L. Wang and C. Fan, *Nat. Commun.*, 2020, **11**, 121.
39 B. Fresch, M. Cipolloni, T.-M. Yan, E. Collini, R. D. Levine and F. Remacle, *J. Phys. Chem. Lett.*, 2015, **6**, 1714–1718.
40 R. Orbach, F. Remacle, R. D. Levine and I. Willner, *Chem. Sci.*, 2014, **5**, 1074.
41 H. Su, J. Xu, Q. Wang, F. Wang and X. Zhou, *Nat. Commun.*, 2019, **10**, 5390.
42 S. Chen, Z. Xu, W. Yang, X. Lin, J. Li, J. Li and H. Yang, *Angew. Chem., Int. Ed.*, 2019, **58**, 18186–18190.
43 W. Li, Y. Yang, H. Yan and Y. Liu, *Nano Lett.*, 2013, **13**, 2980–2988.
44 D. Fan, K. Wang, J. Zhu, Y. Xia, Y. Han, Y. Liu and E. Wang, *Chem. Sci.*, 2015, **6**, 1973–1978.
45 H. Liu, J. Wang, S. Song, C. Fan and K. V. Gothelf, *Nat. Commun.*, 2015, **6**, 10089.
46 G. Chatterjee, N. Dalchau, R. A. Muscat, A. Phillips and G. Seelig, *Nat. Nanotechnol.*, 2017, **12**, 920–927.
47 C. Zhang, J. Yang, S. Jiang, Y. Liu and H. Yan, *Nano Lett.*, 2015, **16**, 736–741.
48 L. Yue, S. Wang, Z. Zhou and I. Willner, *J. Am. Chem. Soc.*, 2020, **142**(52), 21577–21594.
49 G. Men and J.-M. Lehn, *Chem. Sci.*, 2019, **10**, 90–98.

50 G. Vantomme, S. Jiang and J.-M. Lehn, *J. Am. Chem. Soc.*, 2014, **136**, 9509–9518.
51 F. C. Simmel, B. Yurke and H. R. Singh, *Chem. Rev.*, 2019, **119**, 6326–6369.
52 D. Y. Zhang, A. J. Turberfield, B. Yurke and E. Winfree, *Science*, 2007, **318**, 1121–1125.
53 D. Y. Zhang and G. Seelig, *Nat. Chem.*, 2011, **3**, 103–113.
54 A. Amodio, B. Zhao, A. Porchetta, A. Idili, M. Castronovo, C. Fan and F. Ricci, *J. Am. Chem. Soc.*, 2014, **136**, 16469–16472.
55 J.-L. Mergny and D. Sen, *Chem. Rev.*, 2019, **119**, 6290–6325.
56 S. N. Georgiades, N. H. AbdKarim, K. Suntharalingam and R. Vilar, *Angew. Chem., Int. Ed.*, 2010, **49**, 4020–4034.
57 Y. Kamiya and H. Asanuma, *Acc. Chem. Res.*, 2014, **47**, 1663–1672.
58 Y. Kim, J. A. Phillips, H. Liu, H. Kang and W. Tan, *Proc. Natl. Acad. Sci. U. S. A.*, 2009, **106**, 6489–6494.
59 M. W. Haydell, M. Centola, V. Adam, J. Valero and M. Famulok, *J. Am. Chem. Soc.*, 2018, **140**, 16868–16872.
60 R. R. Breaker and G. F. Joyce, *Chem. Biol.*, 1995, **2**, 655–660.
61 M. Famulok, J. S. Hartig and G. Mayer, *Chem. Rev.*, 2007, **107**, 3715–3743.
62 R. J. Lake, Z. Yang, J. Zhang and Y. Lu, *Acc. Chem. Res.*, 2019, **52**, 3275–3286.
63 S. Wang, L. Yue, Z. Shpilt, A. Cecconello, J. S. Kahn, J.-M. Lehn and I. Willner, *J. Am. Chem. Soc.*, 2017, **139**, 9662–9671.
64 L. Yue, S. Wang, V. Wulf, S. Lilienthal, F. Remacle, R. D. Levine and I. Willner, *Proc. Natl. Acad. Sci. U. S. A.*, 2019, **116**, 2843–2848.
65 L. Yue, S. Wang, S. Lilienthal, V. Wulf, F. Remacle, R. D. Levine and I. Willner, *J. Am. Chem. Soc.*, 2018, **140**, 8721–8731.
66 S. Wang, L. Yue, Z. Y. Li, J. Zhang, H. Tian and I. Willner, *Angew. Chem., Int. Ed.*, 2018, **57**, 8105–8109.
67 Z. Zhou, L. Yue, S. Wang, J.-M. Lehn and I. Willner, *J. Am. Chem. Soc.*, 2018, **140**, 12077–12089.
68 L. Yue, S. Wang and I. Willner, *J. Am. Chem. Soc.*, 2019, **141**, 16461–16470.
69 L. Yue, S. Wang, V. Wulf and I. Willner, *Nat. Commun.*, 2019, **10**, 4774.
70 Z. Zhou, X. Liu, L. Yue and I. Willner, *ACS Nano*, 2018, **12**, 10725–10735.
71 Z. Zhou, P. Zhang, L. Yue and I. Willner, *Nano Lett.*, 2019, **19**, 7540–7547.
72 R. Orbach, S. Lilienthal, M. Klein, R. D. Levine, F. Remacle and I. Willner, *Chem. Sci.*, 2015, **6**, 1288–1292.
73 L. Yue, V. Wulf, S. Wang and I. Willner, *Angew. Chem., Int. Ed.*, 2019, **58**, 12238–12245.
74 Z. Zhou, J. Wang and I. Willner, *J. Am. Chem. Soc.*, 2020, **143**, 241–251.
75 A. N. Boettiger, B. Bintu, J. R. Moffitt, S. Wang, B. J. Beliveau, G. Fudenberg, M. Imakaev, L. A. Mirny, C.-t. Wu and X. Zhuang, *Nature*, 2016, **529**, 418–422.
76 V. B. E. Thomsen, *J. Chem. Educ.*, 2000, **77**, 173–176.
77 C. Zhang, Y. Zhao, X. Xu, R. Xu, H. Li, X. Teng, Y. Du, Y. Miao, H.-c. Lin and D. Han, *Nat. Nanotechnol.*, 2020, **15**, 709–715.